

## Scissors mode of a rotating Bose-Einstein condensate

Marco Cozzini and Sandro Stringari

*Dipartimento di Fisica, Università di Trento and Istituto Nazionale per la Fisica della Materia, I-38050 Povo, Italy*

Vincent Bretin, Peter Rosenbusch, and Jean Dalibard

*Laboratoire Kastler Brossel,\* 24 rue Lhomond, 75005 Paris, France*

(Received 3 October 2002; published 7 February 2003)

A scissors mode of a rotating Bose-Einstein condensate is investigated both theoretically and experimentally. The condensate is confined in an axisymmetric harmonic trap, superimposed with a small rotating deformation. For angular velocities larger than  $\omega_{\perp}/\sqrt{2}$ , where  $\omega_{\perp}$  is the radial trap frequency, the frequency of the scissors mode is predicted to vanish like the square root of the deformation, due to the tendency of the system to exhibit spontaneous rotational symmetry breaking. Measurements of the frequency confirm the predictions of theory. Accompanying characteristic oscillations of the internal shape of the condensate are also calculated and observed experimentally.

DOI: 10.1103/PhysRevA.67.021602

PACS number(s): 03.75.Hh, 32.80.Lg

Bose-Einstein condensates rotating at high angular velocity exhibit spontaneous breaking of rotational symmetry [1]. This phenomenon, which is the consequence of two-body repulsive interactions, shows up in the occurrence of considerable deformations of the trapped atomic cloud in the plane normal to the rotation axis. These configurations have been recently observed experimentally using a nearly axisymmetric harmonic trap, with a small deformation of the trapping potential rotating around the  $z$  axis [2].

Under such conditions, the collective modes of the system exhibit interesting features. In particular, one mode in the transverse plane (orthogonal to the rotation axis) corresponds to a shape-preserving oscillation of the atomic cloud with respect to the principal axes  $xy$  of the rotating trap. The frequency  $\omega$  of this scissors-type motion is much smaller than the mean transverse trap frequency  $\omega_{\perp}$ . This surprisingly low value originates from the fact that the restoring force of the oscillation is proportional to the small trap deformation, while the moment of inertia of the condensate remains finite due to its considerable deformation. This represents a major difference with respect to the traditional scissors mode [3,4] of a nonrotating condensate where both the restoring force and the moment of inertia vanish in the limit of an axisymmetric trap.

The purpose of this work is to provide both a theoretic and an experimental investigation of the problem. We first derive the relevant equations describing the scissors mode. For a rotation frequency  $\Omega$  larger than the critical value  $\omega_{\perp}/\sqrt{2}$ , we show that the scissors mode frequency  $\omega$  vanishes like the square root of the trap deformation. We then report on the experimental observation of this scissors mode, and we present results which confirm the theoretic predictions with good accuracy.

The atoms of mass  $m$  are confined in the transverse plane by the potential

$$V_{\perp}(x,y) = m(\omega_x^2 x^2 + \omega_y^2 y^2)/2, \quad (1)$$

where  $\omega_{x,y}^2 = \omega_{\perp}^2(1 \pm \epsilon)$ . The  $(x,y)$  coordinates in the rotating frame are deduced from the coordinates in the laboratory frame by a rotation  $\Omega t$  and the trap deformation  $\epsilon$  is positive. A simple description of the collective oscillations of a rotating condensate is provided by the hydrodynamic equations of superfluids evaluated in the rotating frame:

$$\frac{\partial \rho}{\partial t} + \nabla \cdot [\rho(\mathbf{v} - \mathbf{\Omega} \wedge \mathbf{r})] = 0, \quad (2)$$

$$m \frac{\partial \mathbf{v}}{\partial t} + \nabla \left[ \frac{m v^2}{2} + V + g \rho - m \mathbf{v} \cdot (\mathbf{\Omega} \wedge \mathbf{r}) \right] = 0, \quad (3)$$

where  $\rho(\mathbf{r},t)$  is the spatial density,  $\mathbf{v}(\mathbf{r},t)$  is the velocity field in the laboratory frame, and  $\mathbf{\Omega} = \Omega \hat{u}_z$  ( $\hat{u}_z$  unit vector along the  $z$  axis). The harmonic confining potential  $V(\mathbf{r}) = V_{\perp}(x,y) + m \omega_z^2 z^2/2$  is time independent in the rotating frame. The parameter  $g$  characterizes the strength of the interatomic interactions and is related to the  $s$ -wave scattering length  $a$  by  $g = 4\pi \hbar^2 a/m$ . These equations are valid in the Thomas-Fermi limit, where the so-called quantum pressure term can be neglected in Eq. (3) [5]. We shall be interested here in vortex-free solutions for which  $\nabla \wedge \mathbf{v} = 0$ .

Stationary solutions of these equations can be obtained in the form  $\mathbf{v}_0(\mathbf{r}) = \alpha \nabla(xy)$  for the velocity field and  $\rho_0(\mathbf{r}) = [\tilde{\mu} - m(\tilde{\omega}_x^2 x^2 + \tilde{\omega}_y^2 y^2 + \omega_z^2 z^2)/2]/g$  for the density profile. The density profile has the form of an inverted parabola whose parameters  $(\tilde{\mu}, \tilde{\omega}_x, \tilde{\omega}_y)$  are determined in a self-consistent way as a function of  $\Omega$  [1]. The value of the parameter  $\alpha$  is determined by the solution(s) of the cubic equation  $\alpha^3 + \alpha(\omega_{\perp}^2 - 2\Omega^2) + \epsilon \omega_{\perp}^2 \Omega = 0$ . It is related to the deformation  $\delta = \langle y^2 - x^2 \rangle / \langle x^2 + y^2 \rangle$  of the atomic cloud by the simple expression  $\alpha = -\Omega \delta$ . In the present work, we will be interested in the so-called normal branch [1], corresponding to the stationary solutions which can be obtained by an adiabatic increase of the angular velocity of the trap, starting from  $\Omega = 0$  (see Fig. 1). For  $\Omega \geq \omega_{\perp}/\sqrt{2}$ , these so-

\*Unité de Recherche de l'Ecole Normale Supérieure et de l'Université Pierre et Marie Curie, associée au CNRS.

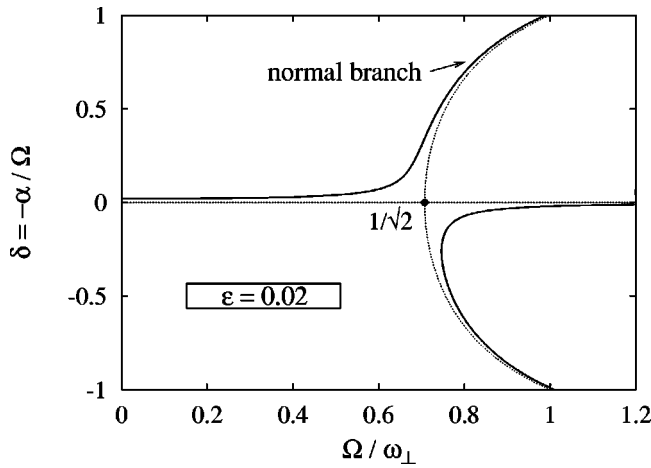


FIG. 1. Deformation  $\delta$  of the cloud for the steady-state solutions of Eqs. (2) and (3) as a function of the angular velocity  $\Omega$  of the trap for a fixed value of the trap deformation  $\epsilon$ . The dotted line represents the solution for  $\epsilon=0$ .

lutions exhibit large values of the cloud deformation ( $\delta \sim 1$ ) even if the trap deformation  $\epsilon$  is much smaller than 1.

An important class of collective oscillations can be derived on top of such stationary configurations by looking for time-dependent solutions of the form

$$\delta\rho(\mathbf{r},t) = a_0 + a_x x^2 + a_y y^2 + a_z z^2 + a_{xy} xy, \quad (4)$$

$$\delta\mathbf{v}(\mathbf{r},t) = \nabla(\alpha_x x^2 + \alpha_y y^2 + \alpha_z z^2 + \alpha_{xy} xy), \quad (5)$$

where  $a_i$  and  $\alpha_i$  are time-dependent parameters to be determined by solving Eqs. (2) and (3). In the linear limit, one can look for solutions varying in time like  $e^{-i\omega t}$ . The collective frequencies in the rotating frame are then found to obey the equation

$$\omega^8 + c_3 \omega^6 + c_2 \omega^4 + c_1 \omega^2 + c_0 = 0, \quad (6)$$

with the coefficients  $c_i$  given in the Appendix. In Ref. [1], it has been shown that these collective oscillations are dynamically stable when evaluated on the normal branch. The stability conditions for higher-multipole oscillations have been studied in Ref. [6], where it has been shown that the normal branch becomes dynamically unstable against the production of such excitations for  $\Omega \geq 0.8\omega_\perp$  when  $\epsilon \rightarrow 0$ .

The solutions of Eq. (6) correspond to four different modes. In particular, for  $\Omega=0$ ,  $\epsilon=0$ , one recovers the well-known  $m = \pm 2$  transverse quadrupole and the two  $m=0$  hybrid quadrupole-monopole modes of a cigar-shaped condensate [7]. The situation changes in the presence of a rotating deformed trap. In fact, one finds that when evaluated on the normal branch (see Fig. 1), the coefficient  $c_0$  in Eq. (6) vanishes linearly as  $\epsilon \rightarrow 0$ , provided  $\Omega > \omega_\perp / \sqrt{2}$ . This gives rise to a soft mode with frequency [9]

$$\omega^2 = -\frac{c_0}{c_1} = \frac{10\omega_\perp^2 \Omega (\omega_\perp^2 - \Omega^2) \sqrt{2\Omega^2 - \omega_\perp^2}}{3\omega_\perp^4 + 3\omega_\perp^2 \Omega^2 + 2\Omega^4} \epsilon. \quad (7)$$

The other three solutions of Eq. (6) instead remain finite for all values of  $\epsilon$  and  $\Omega$ . It is worth noticing that result (7) does not depend on the value of  $\omega_z$ . By looking at the form of the solution for  $\delta\rho$  and  $\delta\mathbf{v}$ , one can show that the soft oscillation (7) corresponds to a scissors mode, i.e., to the oscillation of the angle  $\theta$  between the axes of the condensate and the principal axes  $x, y$  of the trap in the rotating frame. The oscillation of  $\theta$  is accompanied by an oscillation of the condensate deformation  $\delta$  around the equilibrium value  $\delta_0$ . This oscillation of  $\delta$  is dephased by  $\pi/2$  with respect to the one of the angle  $\theta$ . For small trap deformations, we find

$$\delta(t) - \delta_0 = \frac{\omega_\perp^2 \theta}{\Omega^2 \sqrt{2\Omega^2 - \omega_\perp^2}}. \quad (8)$$

The fact that the frequency (7) exactly vanishes when  $\epsilon = 0$  reflects the occurrence of spontaneous breaking of rotational symmetry. For  $\Omega > \omega_\perp / \sqrt{2}$ , the shape of the condensate on the normal branch is indeed deformed even in the limit of a rotationally invariant Hamiltonian (see dotted line in Fig. 1). Since for  $\epsilon=0$  all angles  $\theta$  are equivalent, the oscillation frequency of the condensate around any particular value  $\theta_0$  must vanish. This behavior deeply differs from the scissors mode in a nonrotating condensate. In this case, the deformation of the condensate vanishes when the anisotropy of the static trap tends to zero. Consequently, the frequency of the static scissors mode does not have to vanish in the limit of a symmetric trap; it actually takes the value  $\sqrt{2}\omega_\perp$  [3]. For a fixed anisotropy  $\epsilon \ll 1$ , the scissors frequency calculated in the rotating frame decreases quasilinearly from the value  $\sqrt{2}\omega$  at  $\Omega=0$ , to a value  $\omega \ll \omega_\perp$  at  $\Omega = \omega_\perp / \sqrt{2}$ . For  $\Omega > \omega_\perp / \sqrt{2}$ , it then connects to the value given by Eq. (7).

Result (7) holds for a small amplitude  $\Delta\theta$  of the oscillatory motion of  $\theta$ . To study motions with a larger amplitude, one has to solve numerically the hydrodynamic equations (2) and (3). Using *Ansätze* (4) and (5), we find that the frequency of the motion decreases as  $\Delta\theta$  increases, as for a simple gravitational pendulum.

We now turn to the experimental observation of this scissors mode. We use a  $^{87}\text{Rb}$  gas in a Ioffe-Pritchard magnetic trap, with frequencies  $\omega_x/2\pi = 182$  Hz,  $\omega_y \approx \omega_x$ , and  $\omega_z/2\pi = 11.7$  Hz. The cloud is precooled using optical molasses to a temperature  $\sim 100$   $\mu\text{K}$ . The gas is further cooled by radio-frequency evaporation to a temperature around 50 nK, corresponding to a quasipure condensate with  $10^5$  atoms. We denote by  $t_0$  the time at which the evaporation phase ends. For time  $t > t_0$ , the atomic cloud is stirred by a focused laser beam of wavelength 852 nm and waist  $w_0 = 20$   $\mu\text{m}$ , whose position is controlled using acousto-optic modulators [2]. This laser beam creates a rotating optical-dipole potential that is harmonic over the extension of the cloud. The superposition of this dipole potential and the magnetic one creates a transverse trapping potential identical to Eq. (1). The trap deformation  $\epsilon$  is proportional to the laser intensity  $I_L$  and can be adjusted between 0 and 4%.

The displacement of the center of the trap due to gravity and slight asymmetries in the trapping geometry produce an additional static deformation which has been estimated to be  $\sim 1\%$  by measuring the splitting between the center-of-mass

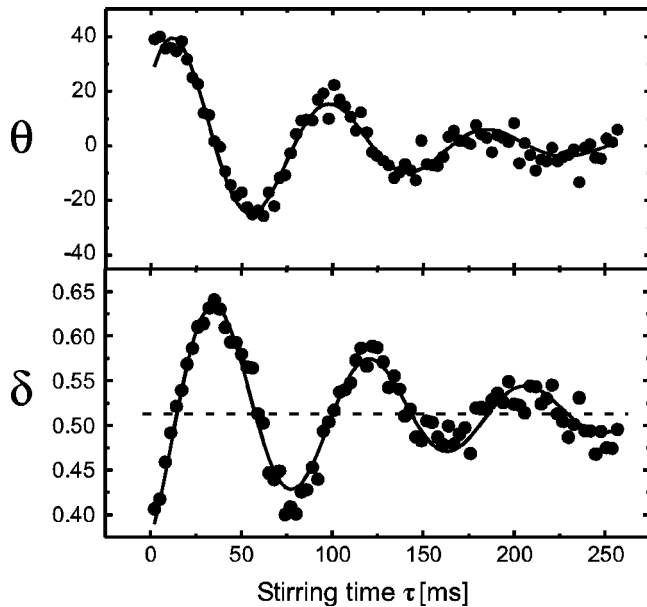


FIG. 2. Variation of the angle  $\theta$  (in degrees) and of the condensate deformation  $\delta$  with the stirring time  $\tau = t_2 - t_1$ . The oscillations of  $\theta$  and  $\delta$  are a signature of the scissors mode. The oscillation frequency  $\omega/2\pi \approx 11.6$  Hz is much smaller than the transverse trap frequency  $\omega_{\perp}/2\pi$ , in agreement with Eq. (7). The solid lines are a fit to the data with a damped sine function. The dashed line in the lower graph shows the stationary value  $\delta = \delta_0$ .

frequencies along the  $x$  or  $y$  axes. This static anisotropy plays a minor role in the present study and has been neglected in the analysis above.

The frequency  $\Omega(t)$  of the stirrer is first varied linearly during the time interval  $(t_0, t_1)$ , starting from  $\Omega(t_0) = 0$  up to  $\Omega(t_1) = 2\pi \times 139$  Hz [so that  $\Omega(t_1) \sim 0.76\omega_{\perp}$ ]. The stirring frequency then stays constant in the time interval  $(t_1, t_2)$ . At time  $t_2$ , we switch off the magnetic trap and the laser stirrer, allow for a 25-ms free fall, and image the absorption of a resonant laser beam propagating along  $z$ . We measure in this way the transverse density profile of the atom cloud, which we fit assuming a parabolic shape. We extract from the fit long and short diameters in the transverse plane [hence, the deformation  $\delta(t)$ ] and the orientation  $\theta(t)$  of the condensate axes with respect to the rotating frame of the laser stirrer.

The excitation of the scissors mode arises directly from the small nonadiabatic character of the condensate evolution as  $\Omega(t)$  increases, during the time interval  $(t_0, t_1)$ . At time  $t_1$ , the state of the condensate slightly differs from the steady state corresponding to  $\Omega(t_1)$ . Consequently, the state of the condensate still evolves in the rotating frame in the time interval  $(t_1, t_2)$ , even though the characteristics of the stirrer do not change anymore.

We have plotted in Fig. 2 the angle  $\theta$  and the condensate deformation  $\delta$  as a function of the time  $\tau = t_2 - t_1$ . These data have been obtained for a ramping time  $t_1 - t_0 = 360$  ms and a spoon anisotropy  $\epsilon = 0.017(6)$ . The angle  $\theta$  oscillates with a frequency  $\omega/2\pi = 11.6(\pm 0.1)$  Hz, in a good agreement with the value  $11.4(\pm 2.1)$  Hz expected from Eq. (7). The initial amplitude  $\Delta\theta$  is  $43^\circ$ , and the oscil-

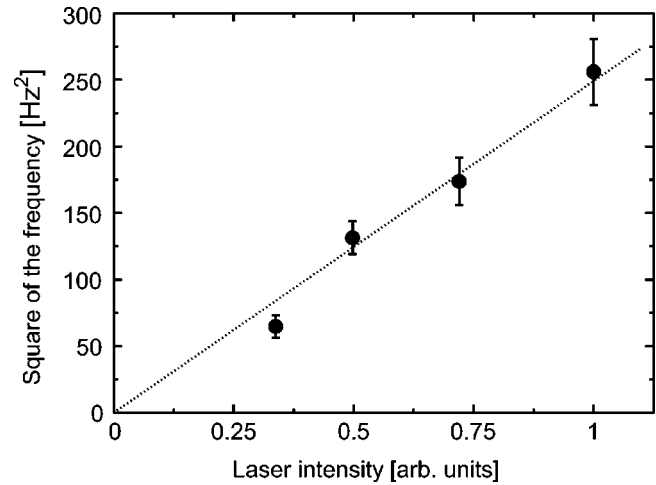


FIG. 3. Variation of the square of the scissors-mode frequency  $\omega/2\pi$  with the laser intensity  $I_L$  (arbitrary units). The error bars indicate the statistical spread of the results obtained for various runs of the experiment. The dotted line is a linear fit according to the prediction of Eq. (7).

lation is damped with a time constant  $\sim 110$  ms. The deformation  $\delta$  of the condensate also exhibits a small oscillatory motion with an amplitude  $\Delta\delta = 0.16$  around the mean value  $\delta_0 = 0.51$ . This motion has the same frequency as that of  $\theta$ , is phase shifted by  $\sim \pi/2$ , as expected from Eq. (8) for the scissors mode, and it is damped with a similar time constant.

To confirm that the oscillatory motion shown in Fig. 2 indeed corresponds to the scissors mode described above, we have measured the variation of the frequency  $\omega$  as a function of the laser intensity, which is itself proportional to the trap anisotropy  $\epsilon$ . The data are plotted in Fig. 3. They clearly show the expected dependence  $\omega^2 \propto \epsilon$ . Actually, this scissors mode constitutes a very precise way to measure  $\epsilon$ , once the frequencies  $\omega_{\perp}$  and  $\Omega$  are known with sufficient precision.

We have also compared the measured amplitudes  $\Delta\theta(t_2)$  and  $\Delta\delta(t_2)$  with the results from a numerical integration of the equations of motion for the coefficients  $a_i$  and  $\alpha_i$  when  $\Omega$  is ramped from 0 up to its final value  $\Omega(t_1)$ . The calculated results reproduce the behavior found experimentally. The amplitude of the scissors mode decreases when the ramping time  $t_1 - t_0$  or the trap anisotropy  $\epsilon$  are increased. The physical reason for this variation is clear: the evolution of the condensate during the time interval  $(t_0, t_1)$  is closer to adiabatic following, and the condensate is left at time  $t_1$  in a state closer to the stationary state expected for  $\Omega = \Omega(t_1)$ . However, we could not reach a strict quantitative agreement between the calculated amplitudes and the measured ones (typical deviation of 50%). We think that this is due to the damping of the scissors mode, present in the experiment (see Fig. 2) and neglected in our simple theoretical model. A proper description of this damping could be obtained using a formalism similar to Ref. [8], where the damping of the scissors mode in a static trap is investigated.

Our final study concerns the behavior of the ratio  $\Delta\delta/\Delta\theta$  at  $t_2$ , where  $\Delta\delta$  and  $\Delta\theta$  are the oscillation amplitudes for the deformation and for the angle, respectively. The results, plotted in Fig. 4, show that  $\Delta\delta/\Delta\theta$  varies linearly with  $\omega/2\pi$

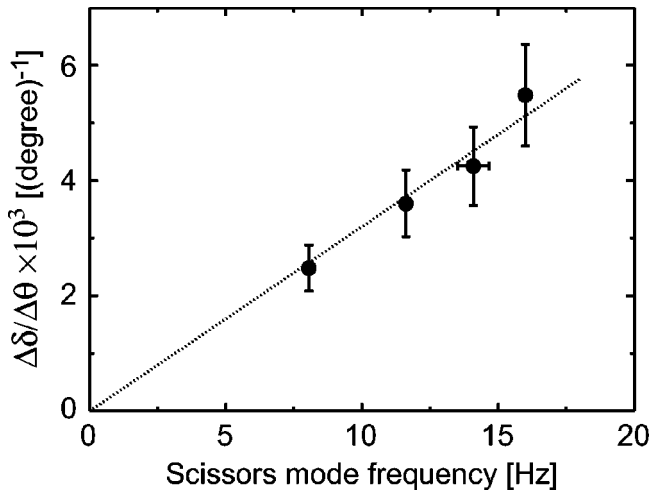


FIG. 4. Variation of the ratio  $\Delta\delta/\Delta\theta$  as a function of  $\omega/2\pi$ . The point with a horizontal error bar corresponds to the average of three results with very similar scissors frequencies  $\omega$ . For small  $\omega$ , corresponding to  $\epsilon \rightarrow 0$ , the oscillation of the cloud deformation is negligible and the condensate motion is similar to that of a rigid body. The dotted line is a linear fit to the data.

with a slope of  $3.2 \times 10^{-4} \text{ (deg Hz)}^{-1}$  [i.e.,  $\Delta\delta/(\omega\Delta\theta) \approx 2.9 \times 10^{-3} \text{ s/radian}^2$ ]. This is in good agreement with the prediction of Eq. (8) that gives an expected slope of  $4.0 \times 10^{-4} \text{ (deg Hz)}^{-1}$ . The small deviation between predicted and experimental slopes may be due to nonlinearities originating from the relatively large amplitude of the excitation. This linear dependence of  $\Delta\delta/\Delta\theta$  on the scissors frequency confirms the idea that for almost symmetric traps, where  $\epsilon \rightarrow 0$  and thus  $\omega \rightarrow 0$ , the motion of the condensate is shape preserving, similar to that of a rigid body.

To summarize, in this paper, we have presented the theoretic analysis and the experimental observation of a scissors mode of a trapped rotating condensate. The existence of this mode relies upon the breaking of the rotational symmetry of the condensate caused by atom interactions. The rotating condensate can have a sizable deformation even in the limit

of an arbitrarily small stirring potential, and this gives unique properties to the mode of interest, such as a frequency much smaller than the trap frequency. Here, we have been mostly interested in the small oscillations of the condensate around its rotating steady state. A natural extension of this work consists in studying the nonlinear regime of the system, where a chaotic dynamics can emerge.

P.R. acknowledges support by the Alexander von Humboldt-Stiftung and by the EU, Contract No. HPMF-CT-2000-00830. S.S. would like to thank the Laboratoire Kastler Brossel for their hospitality. This work was partially supported by the Région Ile de France, CNRS, Collège de France, DRED, and the EU, Contract No. HPRN-CT-2000-00125; and by the Ministero dell'Università e della Ricerca Scientifica e Tecnologica (MURST).

#### APPENDIX

The values of the coefficients  $c_i$  entering into Eq. (6) are

$$c_3 = -\omega_{\perp}^2 \{8(1 + \tilde{\Omega}^2) + 3\lambda^2\},$$

$$c_2 = \omega_{\perp}^4 \{4(5 - 2\epsilon^2) + 16\tilde{\Omega}^2 + 16\tilde{\Omega}^4 - 4[\tilde{\alpha}^2(2\tilde{\Omega}^2 - 1) - 3\tilde{\alpha}\tilde{\Omega}\epsilon] + 2\lambda^2(11 - \tilde{\alpha}^2 + 12\tilde{\Omega}^2)\},$$

$$c_1 = -\omega_{\perp}^6 \{16[(2\tilde{\Omega}^2 - 1)(2\tilde{\Omega}^2 - 1 + \epsilon^2) - \tilde{\alpha}^2(2\tilde{\Omega}^2 - 1 + 3\epsilon^2) - \tilde{\alpha}\tilde{\Omega}\epsilon(5 - 4\tilde{\Omega}^2) - 3\tilde{\Omega}^2\epsilon^2] + 4\lambda^2[(13 - 5\epsilon^2) + 8\tilde{\Omega}^2 + 12\tilde{\Omega}^4 - \tilde{\alpha}^2(2\tilde{\Omega}^2 - 1) + 3\tilde{\alpha}\tilde{\Omega}\epsilon]\},$$

$$c_0 = \omega_{\perp}^8 \{40\lambda^2[(2\tilde{\Omega}^2 - 1)(2\tilde{\Omega}^2 - 1 + \epsilon^2) - \tilde{\alpha}^2(2\tilde{\Omega}^2 - 1 + 3\epsilon^2) - \tilde{\alpha}\tilde{\Omega}\epsilon(5 - 4\tilde{\Omega}^2) - 3\tilde{\Omega}^2\epsilon^2]\},$$

where we have introduced the reduced quantities  $\tilde{\Omega} = \Omega/\omega_{\perp}$ ,  $\lambda = \omega_z/\omega_{\perp}$  and  $\tilde{\alpha} = \alpha/\omega_{\perp}$ .

[1] A. Recati, F. Zambelli, and S. Stringari, *Phys. Rev. Lett.* **86**, 377 (2001).  
 [2] K.W. Madison, F. Chevy, V. Bretin, and J. Dalibard, *Phys. Rev. Lett.* **86**, 4443 (2001).  
 [3] D. Guéry-Odelin and S. Stringari, *Phys. Rev. Lett.* **83**, 4452 (1999).  
 [4] O.M. Maragò, S.A. Hopkins, J. Arlt, E. Hodby, G. Hechenblaikner, and C.J. Foot, *Phys. Rev. Lett.* **84**, 2056 (2000).

[5] F. Dalfovo, S. Giorgini, L. Pitaevski, and S. Stringari, *Rev. Mod. Phys.* **71**, 463 (1999).  
 [6] S. Sinha and Y. Castin, *Phys. Rev. Lett.* **87**, 190402 (2001).  
 [7] S. Stringari, *Phys. Rev. Lett.* **77**, 2360 (1996).  
 [8] B. Jackson and E. Zaremba, *Phys. Rev. Lett.* **87**, 100404 (2001).  
 [9] The same result for  $\omega^2$ , but with negative sign, is obtained for the opposite branch, revealing explicitly its dynamic instability.